

A diffusion hardware phantom looking like a coronal brain slice

C. Poupon¹, L. Laribiere¹, G. Tournier¹, J. Bernard¹, D. Fournier¹, P. Fillard¹, M. Descoteaux², and J-F. Mangin¹
¹CEA I2BM NeuroSpin, Gif-sur-Yvette, F91191, France, ²Université de Sherbrooke, Sherbrooke, Quebec, Canada

Introduction

Diffusion-weighted imaging has become an established technique to infer the micro-structure of the brain. Its more popular application, fiber tractography, is still the only possibility to infer *in vivo* the structural connectivity of the brain. Despite the plethora of available tractography algorithms in the literature, it is still almost impossible to validate them or the local modeling of the angular distribution of fibers *in vivo*. Animal validations remain limited as the injection of virus can be done on a limited set of seeds at once [1][2]. Several hardware phantoms were developed in the past as an alternative to validation using brain tissues [1][3][4][5][6][7], even if their "microstructure" remains simple compared to living tissues. In this work, we present a novel hardware phantom dedicated to the validation of high angular resolution diffusion imaging (HARDI) and tractography algorithms. Its geometry was designed to mimic a coronal slice location of a human brain at the level of the cortico-spinal pathways, depicting a large set of specific configurations (crossings, kissings, splittings, U-fibers).

Material and methods

Mechanical design - The design of the hardware phantom relies on the technology described in [7]. Two negative and positive mediums made from polyurethane acrylic (Fig (b)) were manufactured to represent the shape of the typical fiber bundles contained in a coronal slice of a human brain (Fig (a)). Sheets of cylindrical acrylic fibers (20um in diameter) were carefully interleaved in the negative medium in order to form bundles, crossings, kissings and a U-fiber characterized by a 1cmx1cm cross-section. The sequence for installing of the fiber layers was ordered and defined such that the density of fibers remains constant over the whole phantom and equal to 1900 fibers/mm². A specific container was designed to receive the hardware phantom as well as the pure water solution in which the phantom is immersed (Fig (c)), and a dedicated filling system was used to fill the container under vacuum conditions, in order to prevent any air bubbles to create susceptibility artifacts.

MRI acquisitions - Two high resolution 2D Turbo Spin Echo (TSE) and Gradient Echo (GRE) acquisitions were performed on a Siemens 3T Tim Trio system (Siemens, Erlangen) using a 12-channel head antenna with the following parameters: **TSE** TE/TR=12ms/3s; matrix 384x384; TH=3mm; FOV=192mm; 3 slices (Fig (d)); **GRE** TE/TR=20ms/0.5s; matrix 384x384; TH=3mm; FOV=192mm; 3 slices; flip angle 65°. Diffusion-weighted images (**DWI**) were acquired using three q-space shells at three b-values 650/1500/2000 s/mm², using a single-shot twice refocused spin echo echo-planar (DW-EPI) pulse sequence [8] with the following parameters: TE=77/94/102ms; TR=5s; matrix 64x64; TH=3mm; FOV=192mm; 3 slices; parallel acceleration factor GRAPPA=2; read bandwidth RBW=1775Hz/pixel (Fig (e)).

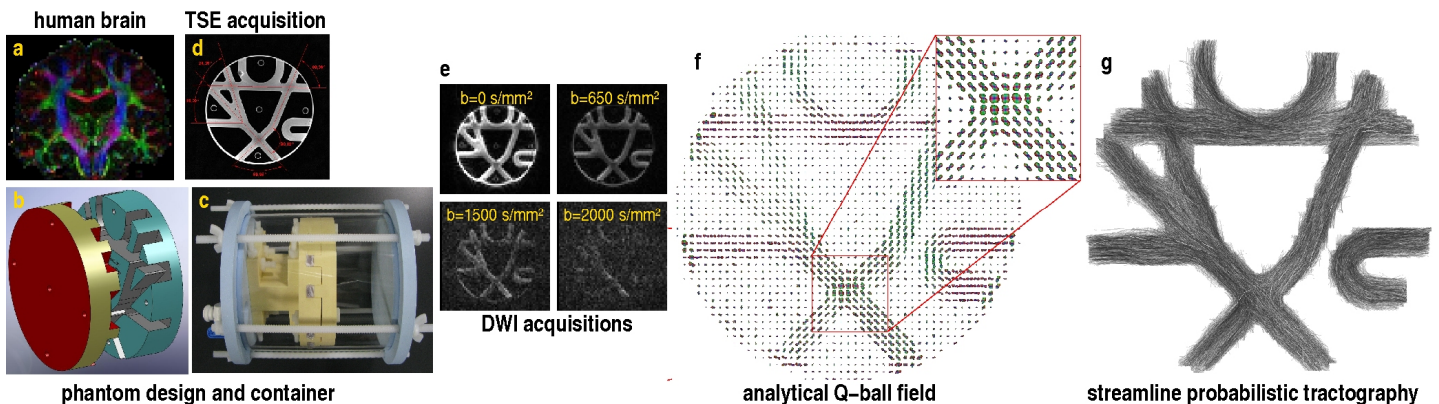
Post-processing - In order to prove that this hardware phantom is suitable for studying and validating local modelings of the diffusion process as well as tractography algorithms, we focused our study on the analytical Q-ball model (QBI) published in [9] to build a field of the orientation distribution functions (ODF) using a maximum spherical harmonic order 6 with a regularization factor 0.006. Then, a streamline probabilistic tractography (SPT) as described in [10] was launched from 27 uniformly distributed seeds per voxel contained in a pre-processed binary mask of the fiber bundles, using an aperture angle of 45° and a forward step of 0.5mm. Of course, this hardware phantom is not limited to the QBI/SPT combination and can be used to study and validate any ODF model with any tractography algorithm.

Results and discussion

TSE and GRE acquisitions depicted no air bubble in the phantom (Fig (d)), allowing the use of an EPI diffusion-weighted pulse sequence. No geometrical distortions could be observed on the DW data (Fig (e)) since no air/bundle interface was present in the phantom thus preventing susceptibility artifacts, and because the twice refocused diffusion sensitization module helped compensating the short time Eddy currents. Consequently, no specific distortion correction was required. Spin echo and inversion recovery spin echo sequences were used to measure the values of the relaxation times: T₂~100ms and T₁~2.4s. The mean apparent diffusion coefficient and fractional anisotropy were estimated to ADC=2.1s/mm² and FA=0.1~0.2. The ADC is three times the average value found in the white or gray matter, suggesting that a maximum b-value of 2000s/mm² in this phantom is equivalent to a maximum b-value of 6000s/mm² in brain tissues, in terms of SNR. Although the FA remains low due to the large diameter of the acrylic fibers, the computed ODFs still depict distinct peaks in regions of crossings, kissings and splittings. Fig (f) depicts a 3D rendering of the analytical Q-ball ODFs and provides a zoom of a region of crossings highlighting the coherence between the peaks of the ODFs and the underlying fiber directions. Fig (g) shows the result of the probabilistic tractography that was able 1) to recover all the fiber bundles present in the hardware phantom, and 2) to adequately deal with the crossing/kissing/splitting configurations.

Conclusion

We have proposed a novel hardware phantom similar to a coronal slice of a human brain, and dedicated to study and validate tractography algorithms as well as HARDI models. Diffusion-weighted images of this phantom were acquired at several b-values on a 3T MRI system. In order to illustrate the suitability of such a phantom for validation, a HARDI model / tractography experiment was performed using a probabilistic algorithm together with an analytical Q-ball HARDI modeling. The data can be freely downloaded at <http://www.inao.fr/spip.php?article112>.



References

- [1] Lin *et al* 2003, NeuroImage 19:482-95
- [2] Campbell *et al* 2005, NeuroImage, 27:725-36
- [3] Perrin *et al* 2005, PTRS 24:1349-61
- [4] Yanasak *et al* 2006, MRI 24:1349-61
- [5] Lorenz *et al* 2005, 13th ISMRM
- [6] Fieremans *et al* 2005, 13th ISMRM
- [7] Poupon *et al* 2008, MRM, 60:1276-83
- [8] Reese *et al* 2003, MRM 49:177-82,
- [9] Descoteaux *et al* 2007, MRM 58:497-510
- [10] Perrin *et al* 2008, Int Journal of Biomed Imaging, Vol 2008